

Intercomparison of smoke aerosol optical thickness derived from GOES 8 imager and ground-based Sun photometers

Jianglong Zhang and Sundar A. Christopher

Department of Atmospheric Science, University of Alabama in Huntsville

Brent N. Holben

Biospheric Sciences Branch, NASA Goddard Space Flight Center, Greenbelt, Maryland

Abstract. Using high temporal resolution GOES 8 imager data and radiative transfer calculations, smoke aerosol optical thickness (τ) is retrieved over selected sites in South America and Central America. The degradation of the signal response in the GOES 8 visible channel is estimated and the satellite-retrieved τ values are then compared against ground-based Sun photometer derived values. The satellite-retrieved values are in good agreement with ground-based τ for two sites in South America with mean linear correlation coefficients of 0.97. For Central America the mean correlation coefficient is 0.80. A single scattering albedo of 0.90 (at 0.67 μm) yields the best agreement between ground-based and satellite retrieved values and is consistent with previous studies. However, our results show that the retrieved optical thickness results are sensitive to single scattering albedo and surface reflectance. For example, a $\pm 3.3\%$ change in single scattering albedo (0.90 ± 0.03) yields an uncertainty in τ of 10% for small optical thickness ($\tau = 0.5$) and an uncertainty of about 25% for larger optical thickness values ($\tau = 1.5$). Although the GOES 8 visible channel has undergone significant degradation in signal response since launch, smoke aerosol optical thickness can be estimated if proper procedures are used to account for this effect.

1. Introduction

Each year more than 100 million tons of smoke aerosols are released into the atmosphere from biomass burning out of which 80% is in the tropical regions [Hao and Li, 1994]. These submicron smoke particles composed primarily of oxidized organic materials are efficient in scattering and absorbing sunlight. There are two major radiative effects of biomass burning aerosols. The first called the "direct" radiative effect refers to the scattering and absorption of incoming solar radiation by smoke aerosols [Penner *et al.*, 1992; Christopher *et al.*, 1996]. The second effect called the "indirect" radiative effect refers to the interaction of smoke aerosols with clouds [Kaufman and Fraser, 1997]. The radiative effect of smoke aerosols on regional and global climate is yet to be understood due to several reasons among which chemical compositions and spatial distributions are critical [Hansen *et al.*, 1997; King *et al.*, 1999; Penner *et al.*, 1992].

One of the key parameters that must be carefully retrieved and studied is smoke aerosol optical thickness (τ) that serves as a measure of aerosol loading in the atmosphere. Currently several ground-based sites from the Aerosol Robotic Network (AERONET) program are in operation to obtain aerosol optical thickness [e.g., Holben *et al.*, 1998]. Satellite retrievals of aerosol optical thickness are limited to ocean

surfaces from NOAA AVHRR data [e.g., Stowe *et al.*, 1997] and dark targets [e.g., Kaufman *et al.*, 1993]. Over land, aerosol index is derived from Total Ozone Mapping Spectrometer (TOMS) measurements [e.g., Hsu *et al.*, 1996] while polarization measurements are used to derive aerosol information [e.g., Deuze *et al.*, 1993].

To date, most satellite retrievals of τ are from polar orbiting satellites such as the AVHRR and LANDSAT. The new generation of GOES imagers [Menzel and Purdom, 1994] on geostationary satellites have improved spatial and spectral capabilities that can be used for cloud [e.g., Greenwald and Christopher, 1999, 2000] and biomass burning fire research [e.g., Prins *et al.*, 1998]. Although biomass-burning fires are routinely studied from GOES imagers [Prins *et al.*, 1998], τ information is still unavailable. One distinct advantage of geostationary satellite data is the high temporal resolution when compared to polar orbiting satellites. This high temporal resolution can be used to obtain information on the diurnal variation of aerosol optical depth. However, due to the degradation in signal response of the visible channel on the GOES imagers [Weinreb *et al.*, 1997], retrieval of geophysical parameters has proven to be a problem.

The major goal of this paper is to use high temporal resolution geostationary data and develop a method to estimate τ from the GOES 8 imager. The satellite-retrieved values are then compared against ground-based measurements. Using the high temporal resolution data set provides for more data points and for evaluating the diurnal variation of aerosol optical thickness.

2. Data and Areas of Study

Half-hourly to hourly data from the GOES 8 imager were used. The imager has channels with half-power response bandwidths of 0.52–0.74 μm (channel 1), 3.79–4.04 μm (channel 2), 6.47–7.06 μm (channel 3), 10.2–11.2 μm (channel 4), and 11.6–12.5 μm (channel 5). The sampled subpoint spatial resolution of channel 1 is 0.57 \times 1 km and for the other channels is 2.3 \times 4.0 km [Menzel and Purdom, 1994].

The total column τ values were obtained from ground-based Sun photometer measurements [Holben *et al.*, 1996, 1998]. The radiances were measured at 340 nm, 380 nm, 440 nm, 500 nm, 670 nm, 870 nm, and 1020 nm and converted to τ at these 7 wavelengths. The τ values used in this paper are obtained after a careful cloud screening process as described by Holben *et al.* [1998] and Smirnov *et al.* [2000]. The uncertainty in ground-based τ values is on the order of 0.01 [Smirnov *et al.*, 2000].

Since the major goal of this paper is to compare satellite retrieved aerosol optical thickness values with ground-based Sun photometer measurements, two sites in South America and one site in the Gulf of Mexico were selected where ground-based Sun photometer measurements were available during 1998. The two sites in South America are Los Fieros (14.6°S, 60.9°W) and Concepcion (16.1°S, 62.0°W). Unfortunately no AERONET measurements were available in Brazil during this time where the majority of biomass burning activities take place [Prins *et al.*, 1998]. For these two locations, hourly GOES 8 data at seven time periods (1344, 1444, 1544, 1644, 1744, 1844 and 1944 UTC) from July–September, 1998 were used. The peak of biomass burning activity is usually in August and September [Prins *et al.*, 1998; Holben *et al.*, 1996]. The month of July was included in the analysis to obtain clear sky estimates of the GOES 8 visible reflectance at each time. During April and May 1998 a large biomass-burning episode was observed from satellites in Central America [Christopher *et al.*, 2000a] and these aerosols were transported to the Gulf of Mexico and northern latitudes. Half-hourly GOES 8 data from five time periods (1401, 1531, 1601, 1901 and 2031 UTC) from April to May 1998 were used to retrieve aerosol optical thickness over Dry Tortugas (24.6°N, 82.8°W) located in the Gulf of Mexico and other selected sites. Table 1 and Table 2 show the latitude and longitude of the Sun photometer sites used in this study. Due to changes in the GOES 8 satellite data collection method, the South America data were at 4-km spatial resolution (subsampling) while the Central America data at 1-km spatial resolution.

Figure 1 shows the region of study and is an example of the smoke aerosols observed from GOES 8 visible imagery. Figure 1a over Central American from May 9, 1998 (1644 UTC) shows the spatial distribution of smoke aerosols from

biomass burning. The smoke aerosols from Mexico were transported to the Gulf of Mexico and were even observed as far as Wisconsin during this episode. The Sun photometer sites are also indicated. Dry Tortugas located downwind from the major fire activities in the Gulf of Mexico had continuous measurements of aerosol optical thickness during April–May 1998. The other sites had limited measurements during this time period (Table 2). Figure 1b from August 24, 1998 (1544 UTC) shows a similar visible imagery from the South America biomass-burning event. Los Fieros and Concepcion, located in Bolivia, consist of mixed forest and agricultural regions and are downwind from major biomass burning regions in Bolivia and Brazil. [Prins *et al.*, 1998; Eck *et al.*, 1999].

Since the GOES 8 retrieved aerosol optical thickness values are compared to the ground-based derived values, these two data sets must be spatially and temporally collocated. To spatially collocate the Sun photometer data with the GOES 8 imager data, a 3X3 array of GOES 8 channel 1 pixels centered on the Sun photometer site was used. This accounts for navigational uncertainties of the GOES 8 imager that are of the order of 2–4 km [Menzel and Purdom, 1994]. To temporally collocate the Sun photometer and satellite data, only GOES 8 data within ± 15 min of the Sun photometer measurements were used. To minimize cloud contaminated GOES 8 imager pixels, the standard deviation within a 3X3 satellite grid box is examined. If the standard deviation of the collocated channel 1 reflectance values within the 3X3 array of pixels is greater than 0.01, these pixels are rejected as being cloud contaminated. Although this may reject some smoke pixels, this appears to be a stringent test. Note that in this comparison, the Sun photometer data were already checked for cloud contamination using procedures described by Holben *et al.* [1998] and because the GOES 8 imager has a larger footprint, the additional 3X3 test were used to remove possible cloud contaminated pixels. Table 1 shows the number of data points used in the study. A total of 1130 points were obtained from Los Fieros, Concepcion and Dry Tortugas during the study period. About 42% of the GOES 8 data points (469 points) were filtered out due to lack of temporal collocation between the GOES 8 and Sun photometer data and also due to missing data. About 6% of the GOES 8 data (63 data points) are rejected due to possible cloud contamination even though the Sun photometer reported aerosol optical thickness values. This is due to the different spatial resolutions of the satellite and ground-based instruments. A total of 597 data points are used in this analysis. In addition to these data, Sun photometer measurements (Table 2) from May 15 to May 27, 1998, were used from selected regions over Mexico and the Southern portion of the United States (L. Remer, personal

Table 1. Summary of GOES 8 Images Used in This Study

Site	Latitude	Longitude	Total Point	Test 1	Test 2	Missing Data	Data Used
Los Fieros	14.56°S	60.93°W	424	130	24	0	269*
Concepcion	16.14°S	62.03°W	427	221	27	1	178
Dry Tortugas	24.60°N	82.80°W	279	113	12	4	150

Test1: Number of points rejected due to lack of temporal within ± 15 min of Sun photometer data. Test 2: Number of points rejected due to possible cloud contamination (standard deviation of 3X3 GOES 8 pixels > 0.01).

* One data point rejected on September 16 1998, 1944 UTC because it was an outlier.

Table 2. Location, Latitude, and Longitude of Aerosol Optical Thickness Data Collected from May 15–27, 1998, During the Central America Biomass-Burning Episode

Location	Latitude	Longitude	Number of Points
Aguascalientes	21.70°N	102.30°W	2
Hualtulco	15.76°N	96.26°W	2
Monclova	25.95°N	101.46°W	2
New Orleans	30.33°N	90.04°W	5
Pensacola	30.45°N	87.19°W	3
Others			3

Data were collected at the following UTC times: 1401, 1531, 1601, 1701, 1901, 2001, and 2031. See figure 2 for the locations.

communication, 2000). A total of 17 data points are used for this portion of the analysis (Table 2).

3. Calibration Issues

Channel 1 of the GOES 8 imager was not designed for long-term accurate radiometry and thus has no onboard calibration. The other GOES channels have onboard calibration. Deriving useful quantitative information from satellite sensor measurements requires accurate calibration. All channels of the GOES imagers undergo extensive calibration testing prior to launch [Weinreb *et al.*, 1997]. The visible channel on the GOES imager is more problematic, a channel that was intended to supply more qualitative information. A lack of onboard calibration makes the reliable retrieval of aerosol optical depth more difficult because calibration errors are one of the largest sources of uncertainty in estimating visible optical depth from satellite radiance measurements [Pincus *et al.*, 1997]. This drawback, however, should not preclude the use of GOES visible channel measurements in aerosol property studies. Other studies have accounted for this degradation and successfully performed cloud property retrievals using GOES imager data [e.g., Greenwald and Christopher, 1999, 2000; Greenwald *et al.*, 1997].

There have been several attempts to assess and monitor the visible channel calibration through vicarious means [e.g., Bremer *et al.*, 1998; Rao *et al.*, 1999; Nguyen *et al.*, 1999]. These studies all report that the GOES 8 imager have undergone signal degradation. This degradation is probably caused by the accumulation of material on the scanning mirror [Ellrod *et al.*, 1998] that may be a result of outgassing. The GOES 8 imager visible channel also suffered an unexpected drop of about 9% in signal response soon after launch [Ellrod *et al.*, 1998]. Based on GOES imager measurements of clear ocean scenes, Knapp and Vonder Haar [2000] have estimated this initial drop in response to be about 10.4%. The subsequent rate of degradation for the GOES 8 imager visible channel has been estimated to be about 5.6% per year (from August 1995 to August 1999) that is consistent with a simple GOES 8/9 intercalibration test used by Greenwald *et al.* [1997]. Therefore, in this study we account for the degradation of the GOES 8 visible channel using the methodology described by Knapp and Vonder Haar [2000]. This method compares raw counts of clear ocean scenes to theoretical satellite-detected radiance values from a radiative transfer model that is similar to the procedure used by Fraser

and Kaufman [1986]. Vicarious calibrations were performed at 6-month intervals beginning August 1995 to August 1999.

4. Method

The radiance observed by a satellite sensor is composed of contributions from the atmosphere and the surface. In cloud-free areas, the radiance contribution from the atmosphere includes both Rayleigh and aerosol scattering. The radiance received at the sensor from the surface includes the light reflected by the surface that is directly transmitted to the sensor and the light reflected by the surface and scattered by the atmosphere into the sensor.

A discrete ordinate radiative transfer (DISORT) model [Ricchiazzi *et al.*, 1998] is used to pre-calculate the satellite measured spectral radiance as a function of aerosol optical depth, sun-satellite viewing geometry and surface albedo. A tropical atmospheric profile of pressure, temperature, water vapor, and ozone density is used [McClatchey *et al.*, 1972]. Therefore, for a given satellite visible channel radiance and a known sun-satellite view geometry an aerosol optical thickness value can be obtained from pre-computed tables. However, this method requires knowledge of aerosol properties such as aerosol size distribution and refractive index. Values of surface albedo are also required for simulating the satellite observed radiance. A Lambertian surface is assumed and surface reflectivity is obtained for each time period by obtaining the minimum top of atmosphere (TOA) radiance over a 30-day period when aerosol concentrations are low (July). For example over Los Fieros, from July 1998 a clear sky value is obtained for each one of the seven time periods from 1344 to 1944 UTC. The TOA values are then converted to surface values using radiative transfer calculations. The mean (over all hours) TOA GOES 8 visible channel clear sky reflectance for Los Fieros, Concepcion and Dry Tortugas were $8 \pm 0.6\%$, $9.2 \pm 0.5\%$, and $3.9 \pm 0.2\%$, respectively. The corresponding surface albedos were $5.7 \pm 0.4\%$, $7.2 \pm 0.5\%$, and $1.5 \pm 0.1\%$. The sensitivity of the results to different surface albedos is discussed in section 5.

In this study, smoke aerosols were characterized as spheres that are well supported by previous studies [Martins *et al.*, 1998]. Therefore Mie calculations were performed to obtain the scattering and absorbing properties of aerosols. The biomass burning aerosols are characterized as an internal mixture of black carbon core surrounded by an organic shell [McDow *et al.*, 1996; Ross *et al.*, 1998]. A lognormal size distribution is assumed with an average volume mean diameter of $0.3 \mu\text{m}$ [Anderson *et al.*, 1996; Reid *et al.*, 1998b] and a standard deviation of 1.8 [Reid *et al.*, 1998b; Remer *et al.*, 1998]. The densities of the black carbon core and the organic shell were assigned values of 1.8 g cm^{-3} and 1.2 g cm^{-3} respectively [Ross *et al.*, 1998]. The real part of the refractive index of the shell ranges from 1.4 to 1.6 [D'Almeida *et al.*, 1991; Martins *et al.*, 1998; Anderson *et al.*, 1996; Remer *et al.*, 1998]. Therefore, for the organic shell, a mean value of 1.5 was used with no absorption [Ross *et al.*, 1998; Reid *et al.*, 1998a]. The real and imaginary part of the refractive index of the black carbon core is assumed to be $1.63-0.48i$ [Chang and Charamampoulos, 1990]. There is a range of mass fraction values of black carbon reported in the literature. Perreira *et al.* [1996] report measured mass

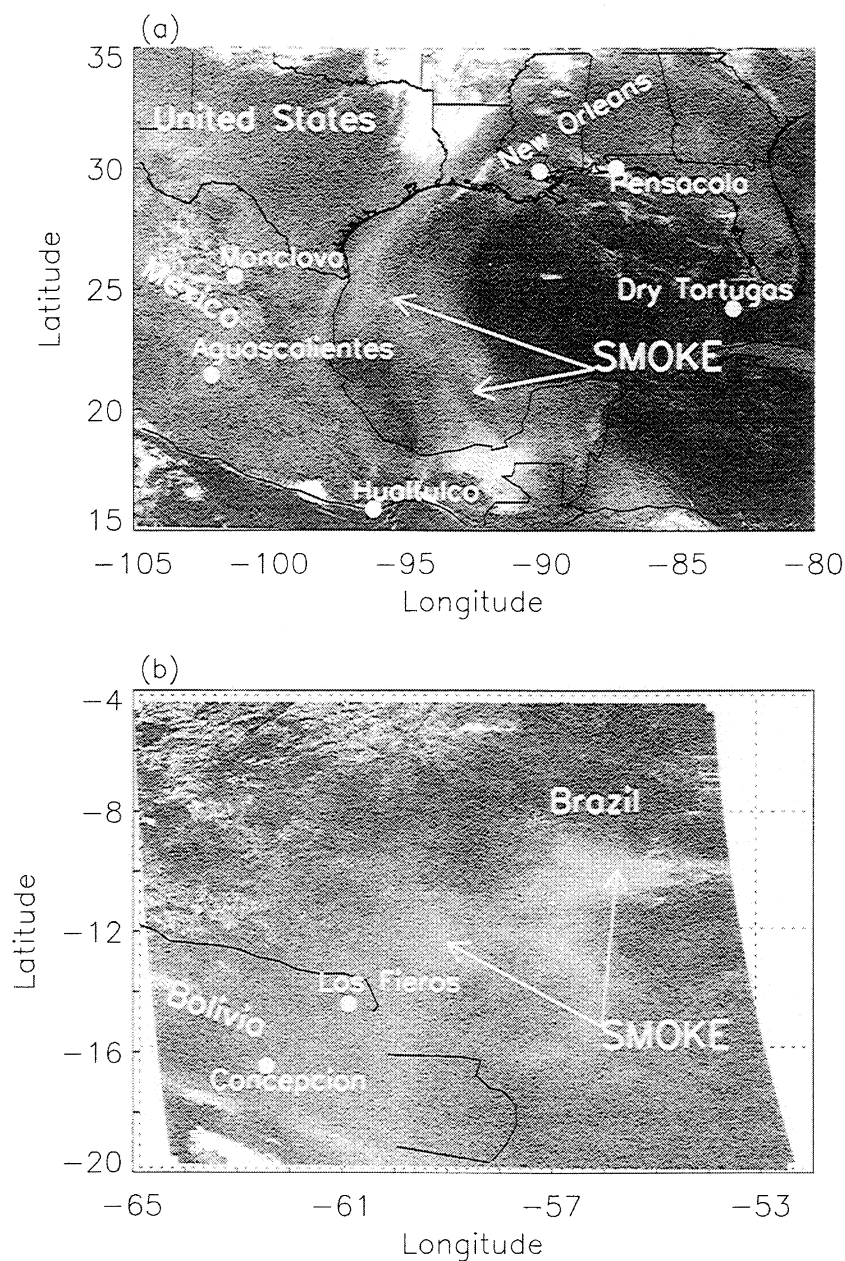


Figure 1. GOES 8 visible imagery denoting area of study and locations of Sun photometer sites: (a) In Central America for May 9, 1998 (1644 UTC), and (b) in South America for August 24, 1998 (1544 UTC).

fraction of black carbon content ranging from 0.4–8.4%. Ferek *et al.* [1998] report values of 5% for smoldering and 7.5% for flaming conditions. Artaxo *et al.* [1998] report values for the black carbon mass concentration as $5.49 \mu\text{g m}^{-3}$ equivalent to 1–7% of aerosol mass load. Other studies report mass fraction values ranging from 5–8% [Reid *et al.*, 1998b], 5–10% [Ross *et al.*, 1998], and 5–11% [Kaufman *et al.*, 1992]. The variation in the mass fraction values is due to the different aerosol sources and age of the smoke [Reid *et al.*, 1999]. In this study, the mass fraction of the black carbon core is assumed to 4.5% that yielded a single scattering albedo (ω_0) of 0.90.

One of the key parameters that affect optical thickness retrievals is ω_0 [e.g., Chu *et al.*, 1998]. Therefore the

sensitivity of the retrieved aerosol optical thickness to ω_0 is examined in section 5. Different values of aerosol single scattering albedo can be obtained by varying any one of several input parameters to the Mie calculations. These parameters are the real and imaginary part of the refractive index, size distribution parameters such as diameter and standard deviation and also the mass fraction of the black carbon core relative the organic shell. To test the sensitivity of the retrieved τ values to ω_0 , we varied the mass fraction of the black carbon core to yield different values of ω_0 . A mass fraction of 3% yielded a value of 0.93 and a mass fraction of 6% yielded a value of 0.87. Other studies have varied the imaginary part of the refractive index to yield different ω_0 values [Chu *et al.*, 1998].

5. Results and Discussion

The two sites in South America (Los Fieros and Concepcion) and one site in the Gulf of Mexico (Dry Tortugas) provided continuous values of ground-based aerosol optical thickness during the study period. Figure 2 shows a scatterplot of the GOES 8 retrieved aerosol optical thickness versus the Sun photometer values for Los Fieros (Figure 2a) and Concepcion (Figure 2b) for an ω_0 value of 0.90. The vertical and horizontal error bars denote the standard deviation in space (GOES 8; 3X3 box) and time (Sun photometer; 15 min). The lack of a horizontal bar indicates that the standard deviation is small. Also shown in the inset of Figures 2a and 2b are the frequency distributions of the Sun photometer and GOES 8 retrieved values for each site. The mean and standard deviation of the GOES 8 and Sun photometer derived τ values for Los Fieros are 0.43 ± 0.45 and 0.49 ± 0.48 , respectively, with a linear correlation coefficient of 0.98. For Concepcion (Figure 2b), the mean and standard deviation of the GOES 8 and Sun photometer τ values are 0.36 ± 0.34 and 0.38 ± 0.38 , respectively, with a linear correlation coefficient of 0.96. There is excellent agreement between the measured and the calculated τ values for these two sites over the study period. More than 70 % of the τ values are below 0.5 for both Los Fieros and Concepcion.

Figures 3a and 3b show the relationship between the Sun photometer and GOES 8 retrieved aerosol optical thickness values for Dry Tortugas and the other selected sites (Table 2) respectively. For Dry Tortugas the mean and standard deviation of the GOES 8 and Sun photometer values are 0.17 ± 0.12 and 0.18 ± 0.10 , respectively, with correlation coefficient of 0.78. The lower correlation coefficient is partly due to the GOES 8 retrieved values estimating larger values of τ when compared to the measured values for 10% of the data points and also due to the smaller range of optical thickness values. For the other selected sites in Mexico and southern United States (Figure 3b), the mean and standard deviation of the GOES 8 and Sun photometer values are 0.76 ± 0.32 and 0.74 ± 0.22 , respectively, with a correlation coefficient of 0.84. There were only 17 data points used for this portion of the analysis. Table 3 provides a summary of the results. The correlation coefficients and the slope and intercept values are shown for each site. Los Fieros and Concepcion are downwind of major biomass burning regions and therefore the optical thickness values are higher than those observed at Dry Tortugas where the majority of the aerosols were transported from the Central American region. The mean values of τ at Dry Tortugas are roughly two to three times smaller than the mean values observed at Los Fieros and Concepcion. Although fixed values of ω_0 were used to retrieve aerosol optical thickness, the aging and transport of aerosols could change ω_0 values that is not accounted for in this study [Reid *et al.*, 1999]. Independent measurements will be needed to account for the variation of aerosol properties with time.

To assess the impact of single scattering albedo on τ retrievals, we varied the mass fraction of the black carbon core from 3-6% to yield different single scattering albedos (0.87-0.93). This range of single scattering albedos is within the range of measurements made during the SCAR-B experiment [Reid *et al.*, 1998a, 1998b]. Figure 4a shows a scatterplot of the GOES 8 retrieved τ for an ω_0 value of 0.90

versus the GOES 8 retrieved τ for ω_0 values of 0.87, 0.90 and 0.93 for 269 points over Los Fieros, Bolivia. This allows us to estimate the uncertainty in τ retrievals if different ω_0 values were assumed instead of a value of 0.90. For small aerosol optical thickness ($\tau=0.5$), a change in ω_0 value from 0.87 to 0.93 will yield τ values ranging 0.55 to 0.44. This leads to an uncertainty in τ of 0.5 ± 0.05 that is of the order of 10%. For larger aerosol optical thickness ($\tau=1.5$), this uncertainty is larger that is of the order of 17 to 32%. For $\tau=1.5$, if an ω_0 value of 0.87 was used instead of 0.90, the retrieved τ is 1.98, leading to an uncertainty of 32%. However, if ω_0 is 0.93, the retrieved τ is 1.24 that is a 17% uncertainty. The uncertainties in retrieved aerosol optical thickness are larger for larger optical thickness when compared to smaller optical thickness values that were also shown from MODIS Airborne Simulator (MAS) data [Chu *et al.*, 1998]. Our analysis shows that for Los Fieros more than 70% of the data have optical thickness less than 0.5, and therefore the uncertainty in retrieved optical thickness is less than 10%.

Figure 4b shows the sensitivity of the GOES 8 retrieved results to the assumed surface albedo. Since surface albedos are required as input to the radiative transfer model, we estimate the uncertainty in the retrieved τ values to assumed surface albedos. Recall that minimum reflectance values were obtained on a pixel-by-pixel basis for each time period over a month to determine clear sky values. These TOA values were converted to surface albedo values using the DISORT model. For the GOES 8 visible channel, the difference in reflectance values between the TOA and the surface are of the order of 2%. Therefore, for each time period a surface albedo value was obtained that was used as input to the radiative transfer calculations to estimate aerosol optical thickness. Using a ω_0 of 0.9, we examined the sensitivity of the τ results to changes in surface albedo. Figure 4b shows that the uncertainties in the GOES 8 retrieved τ values as a function of surface albedo. For example, for small τ values of 0.5, the uncertainty in the retrieved τ values is larger due to a $\pm 1\%$ change in surface albedo when compared to larger values. As τ increases, the contribution from the surface decreases where as for smaller τ , the surface contribution is larger. For smaller τ the uncertainty in the retrieved τ values could be rather large where as for larger τ the uncertainties are on the order of 4%. Therefore accurate characterization of surface reflectance is important in aerosol optical thickness retrievals, especially when aerosol optical thickness is small. We also estimated the sensitivity of the GOES 8 retrieved τ values to the assumed yearly rate of degradation. Recall that a yearly degradation of 5.6% per year was used to adjust the visible channel reflectance values [Knapp and Vonder Haar, 2000]. A $\pm 10\%$ change in the yearly degradation rate yielded a 10% change in τ values for small optical thickness ($\tau=0.5$) and a 7% change in optical thickness for larger τ values ($\tau=1.5$).

To summarize, the retrieved τ values are sensitive to assumed values of ω_0 and surface albedo. For smaller τ values ($\tau < 0.5$), the assumed ω_0 values cause less uncertainty in the retrieved τ values when compared to the surface albedo effects. Therefore these two effects may counteract each other. Similarly, for larger τ value ($\tau > 1.0$), the retrieved τ results values are less sensitive to the assumed surface albedo when compared to the ω_0 values.

Next we examine the time series of GOES 8 retrieved aerosol optical thickness (open circles) over Los Fieros

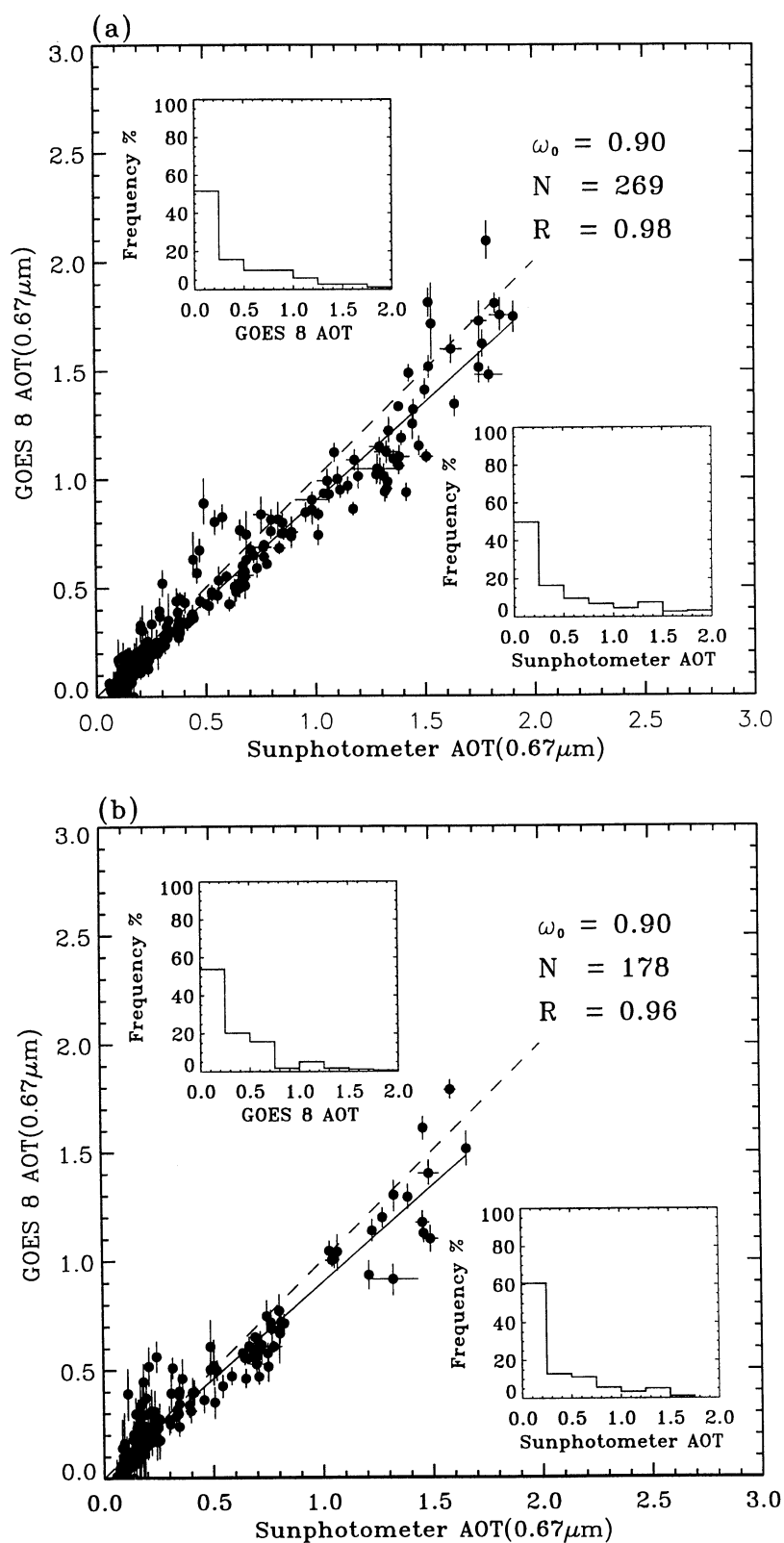


Figure 2. Intercomparison of GOES 8 retrieved aerosol optical thickness and Sun photometer derived values for Bolivia for (a) Los Fieros and (b) Concepcion. The dashed line denotes the one-to-one correspondence, and the solid line is the least squares fit.

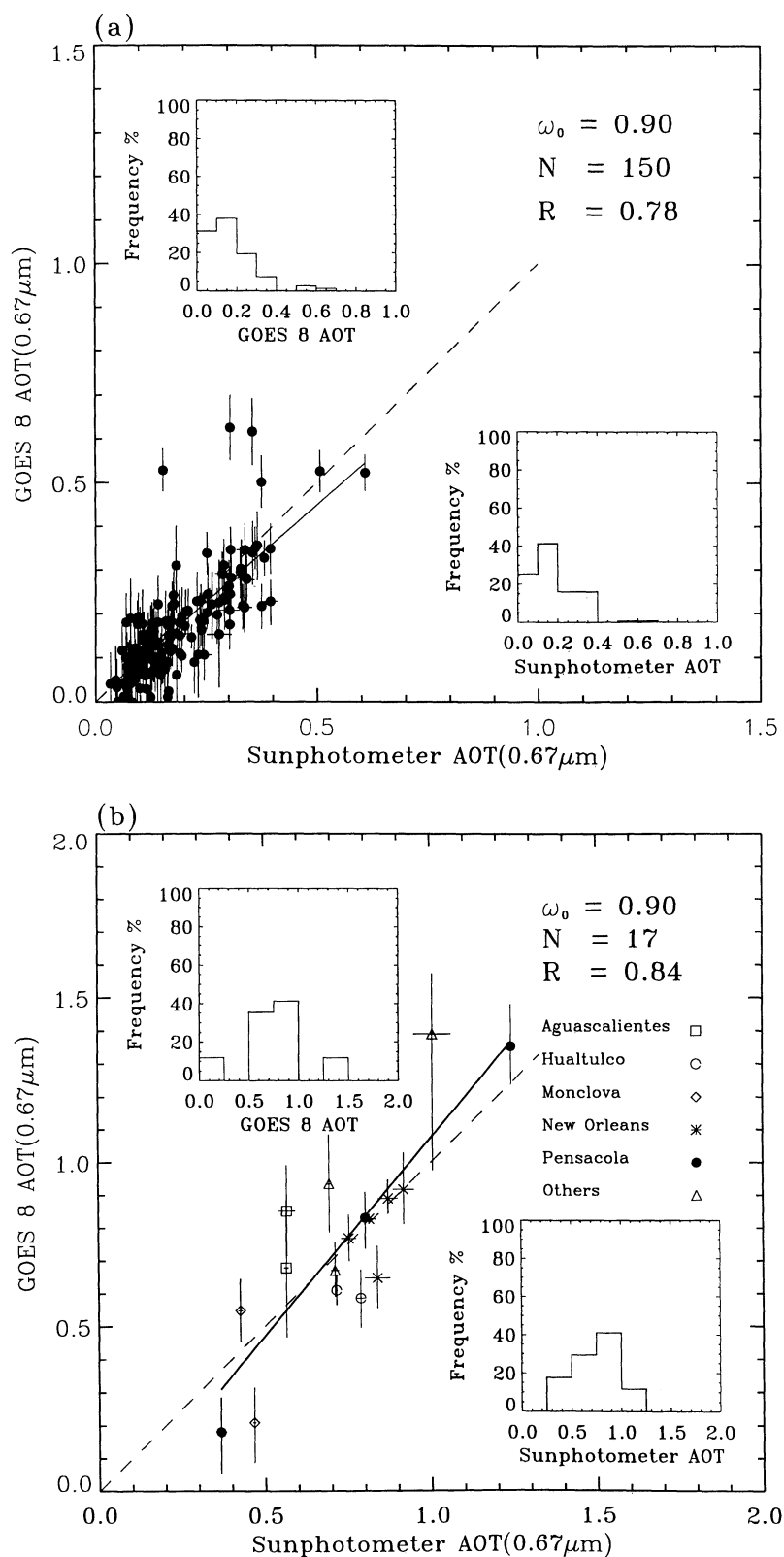


Figure 3. Intercomparison of GOES 8 retrieved aerosol optical thickness and Sun photometer derived values in Central America for (a) Dry Tortugas and (b) other sites (see Table 2). The dashed line denotes the one-to-one correspondence, and the solid line is the least square fit.

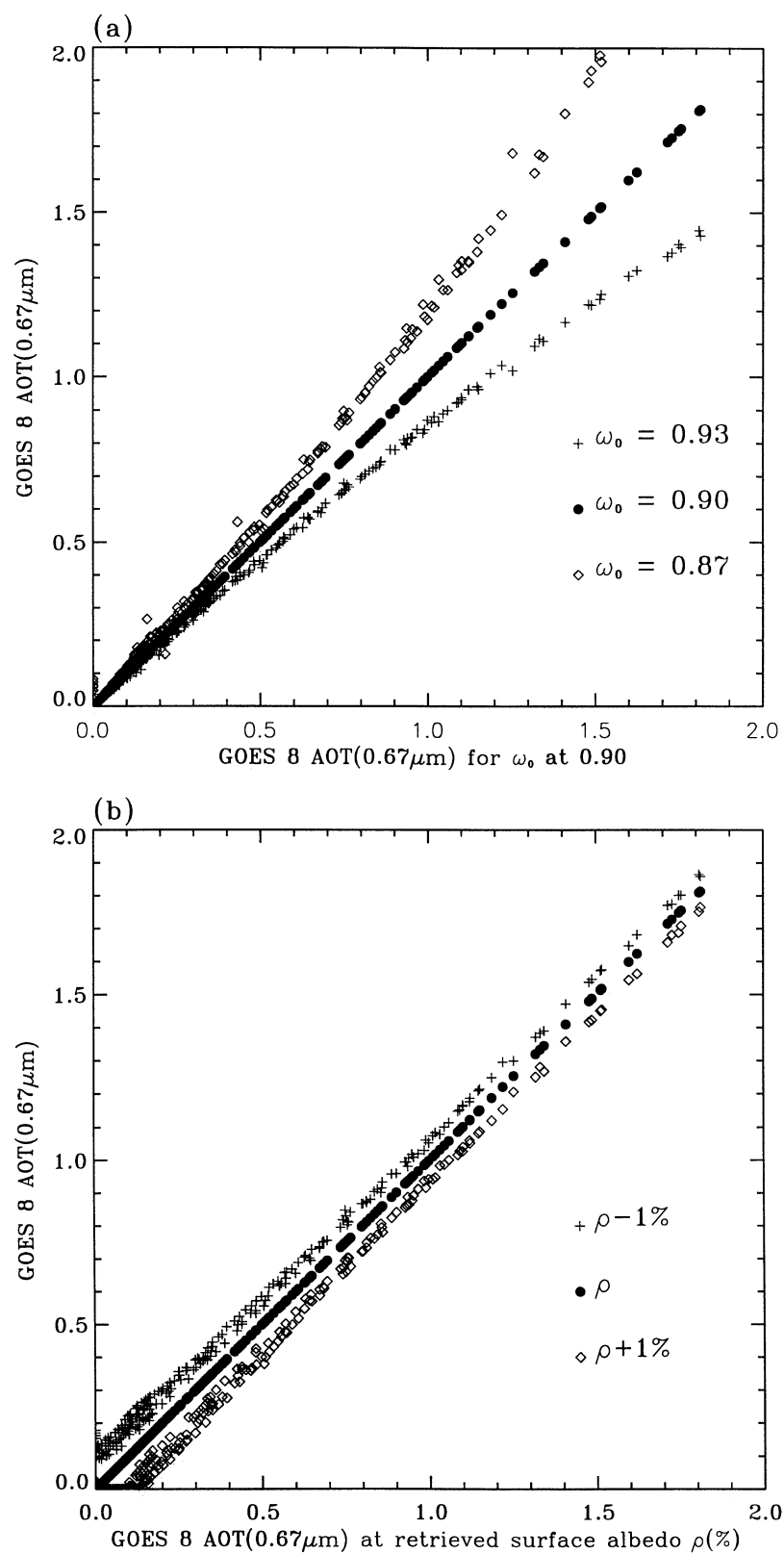


Figure 4. Sensitivity of satellite retrieved aerosol optical thickness to (a) single scattering albedo and (b) surface albedo.

Table 3. Summary of Results From the Study Period

Site	Number of points	GOES 8 τ		AERONET τ		R	Slope	Intercept	ω_0 (0.67 μm)
		μ	σ	μ	σ				
Los Fieros	269	0.43	0.45	0.49	0.48	0.98	0.91	-0.02	0.90
Concepcion	178	0.36	0.34	0.38	0.38	0.96	0.88	0.02	0.90
Dry Tortugas	150	0.17	0.12	0.18	0.10	0.78	0.89	0.01	0.90
Others sites	17	0.76	0.32	0.74	0.22	0.84	1.20	-0.13	0.90

R denotes linear correlation coefficient, and μ and σ denote the mean and standard deviation.

(Figure 5) from July 1 to September 15, 1998 for seven time periods from 1344–1944 UTC on an hourly basis. The points are not connected when there are data gaps. The Sun photometer-derived τ values are also shown (solid circles). The τ values from July 1 to August 1, 1998 are low, of the order of 0.1. The τ values increase from August with peak values of 1.5–2.0 around September 1, 1998, that is during the peak biomass burning activity [Prins *et al.*, 1998; Holben *et al.*, 1996]. The aerosol optical depth at these locations are a combination of regional burning along with transport from areas northeast of these sites where heavy biomass burning takes place each year [Christopher *et al.*, 1998; Prins *et al.*, 1998]. Although fire activities peak in the afternoon, the smoke aerosol optical depths are not necessarily correlated with the fire patterns because of aerosol transport from other regions [Prins *et al.*, 1998]. To examine if there are differences as a function of time, the linear correlation coefficients along with bias and root mean square errors (GOES 8, – Sun photometer retrieved) for each time period

was examined (Table 4). The correlation coefficient is greater than 0.93 for all times except at 1844 UTC for Concepcion due to the slightly smaller optical depths retrieved by the GOES 8 method when compared to the Sun photometer derived values. There mean bias errors for Los Fieros and Concepcion are –0.06 and –0.02, respectively, and the RMS errors are 0.12 and 0.11.

To utilize the full potential of the GOES imagers, the next step is to develop a robust algorithm to separate biomass burning aerosols from clear and cloudy regions and apply the aerosol model from this study to obtain smoke aerosol optical thickness on a regional basis from GOES 8 imagery.

6. Summary

Aerosols play a key role on the radiation balance of the Earth-atmosphere system [King *et al.*, 1999]. Aerosol optical thickness that is a measure of aerosol concentration is one important parameter that is needed to understand the radiative

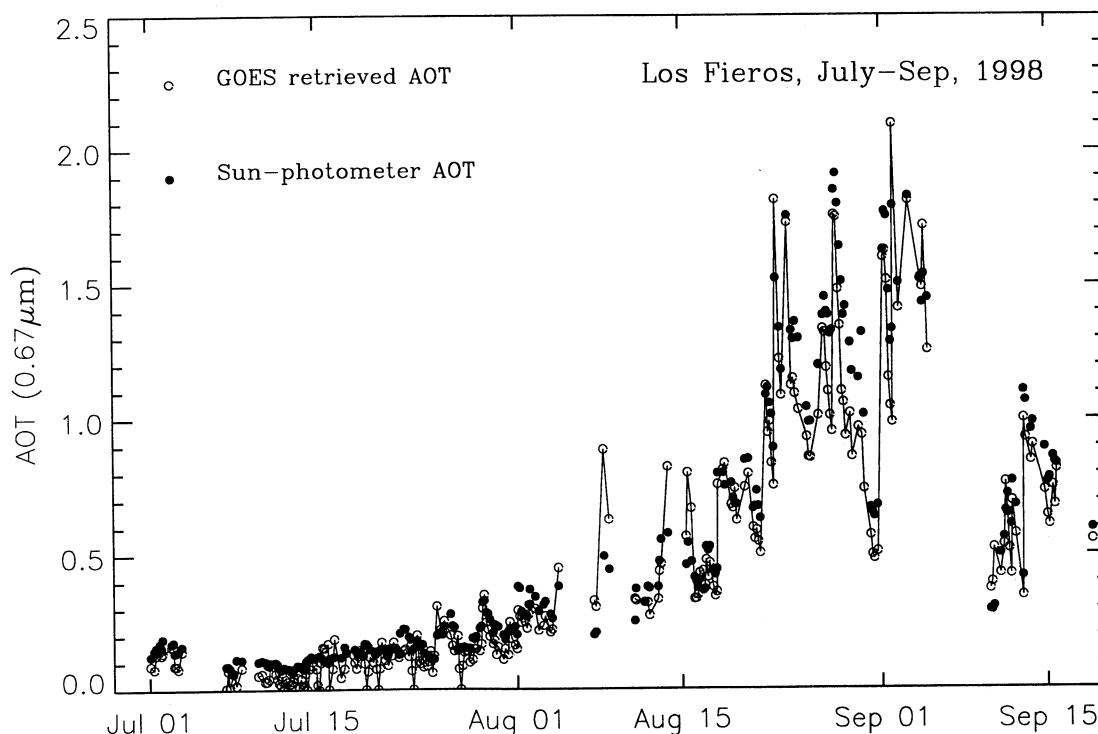


Figure 5. Time series (July 1 to September 18, 1998) of retrieved GOES 8 aerosol optical thickness (open circles) and Sun photometer optical thickness (solid circles) from 1344 to 1944 UTC for Los Fieros.

Table 4. Linear Correlation Coefficients, Bias and Root-Mean-Square Errors Between GOES 8 and Sun Photometer Derived Aerosol Optical Thickness As a Function of Time for Los Fieros (LF) and Concepcion (C)

Time (UTC)	Number of points		R		Bias		RMS	
	LF	C	LF	C	LF	C	LF	C
1344	40	39	0.99	0.99	-0.05	-0.02	0.10	0.07
1444	31	28	0.99	0.97	-0.09	-0.03	0.11	0.10
1544	47	33	0.98	0.97	-0.07	-0.03	0.13	0.10
1644	43	20	0.98	0.94	-0.04	0.03	0.12	0.16
1744	36	19	0.98	0.97	-0.08	-0.09	0.14	0.14
1844	37	21	0.96	0.85	-0.05	-0.03	0.13	0.12
1944	35	18	0.98	0.96	-0.06	-0.04	0.13	0.07
Total/Mean	269	178	0.98	0.96	-0.06	-0.02	0.12	0.11

impact of aerosols both at the TOA [Christopher *et al.*, 2000a] and at the surface [Christopher *et al.*, 2000b]. Due to its superior coverage, satellite remote sensing techniques are especially suited for obtaining the spatial distribution of aerosols and their radiative impact. Most studies have utilized polar orbiting satellite such as AVHRR, LANDSAT, and TOMS to estimate smoke aerosol optical thickness. In this paper we use high temporal resolution GOES 8 imager data to estimate smoke optical thickness from the visible channel. Since the sensitivity of the GOES 8 visible channel has undergone significant degradation since launch, we adjust the visible channel reflectance values based on previous research [Knapp and Vonder Haar, 2000]. The retrieved smoke aerosol optical thickness over selected sites in South America and Central America are compared against ground-based aerosol optical thickness derived from Sun photometer measurements. Using a single scattering albedo of 0.90, our results indicate that there is good agreement between satellite and Sun photometer derived aerosol optical thickness. This value of single scattering albedo is consistent with previous studies [Chu *et al.*, 1998]. Although there is good agreement, we note that the retrievals are sensitive to both single scattering and surface albedo. Surface albedo effects play a larger role at smaller optical depths ($\tau < 0.5$) and single scattering albedo effects are larger at larger optical thickness values. Therefore proper characterization of aerosol and surface properties is necessary. As a next step a reliable smoke detection scheme must be developed from GOES 8 imager data that would allow the estimation of smoke aerosol optical thickness on a regional and global basis. This can then be used to study diurnal variation of smoke optical thickness over large areas that will serve as a valuable tool for aerosol radiative forcing studies.

Acknowledgments. This research was partially supported by NASA grants NAG57270 (TOMS) and NCC 8141 (Global Aerosol Climatology Project) and was part of J. Zhang's Master's thesis. The GOES data were obtained through the Global Hydrology and Climate Center. We thank Ken Voss for the Dry Tortugas Sun photometer data and Lorraine Remer for the ground-based data from Mexico. We thank Udaysankar Nair for providing the GOES calibration code and Xiang Li for his insightful comments. We also thank Warren Wiscombe for the Mie code for stratified spheres.

References

- Anderson, B. E., W. B. Grant, G. L. Gregory, E. V. Browell, J. E. Collins Jr., G. W. Sachse, D. R. Bagwell, C. H. Hudgins, D. R. Blake, and N. J. Blake, Aerosols from biomass burning over the tropical South Atlantic region: Distributions and impacts, *J. Geophys. Res.*, **101**, 24,117-24,137, 1996.
- Artaxo, P., E. T. Fernandes, J. V. Martins, M. A. Yamasoe, P. V. Hobbs, W. Maenhaut, K. M. Longo, and A. Castanho, Large-scale aerosol source apportionment in Amazonia, *J. Geophys. Res.*, **103**, 31,837-31,847, 1998.
- Bremer, J. C., J. G. Baucom, H. Vu, M. P. Weinreb, and N. Pinkine, Estimation of long-term throughput degradation of GOES 8 and 9 visible channels by statistical analysis of star measurements, in *Conference on Earth Observing Systems III*, edited by W. L. Barnes, pp. 145-154, NASA Goddard Space Flight Ctr., Greenbelt, Md., 1998.
- Chang, H., and T. T. Charalampopoulos, Determination of the wavelength dependence of refractive indices of flame soot, *Proc. R. Soc. London, Ser. A*, **430**, 577-591, 1990.
- Christopher, S. A., D. V. Kliche, J. Chou, and R. M. Welch, First estimates of the radiative forcing of aerosols generated from biomass burning using satellite data, *J. Geophys. Res.*, **101**, 21,265-21,273, 1996.
- Christopher, S. A., M. Wang, T. A. Berendes, R. M. Welch, and S. K. Yang, The 1985 biomass burning season in South America: Satellite remote sensing of fires, smoke, and regional radiative energy budgets, *J. Appl. Meteorol.*, **37**, 661-678, 1998.
- Christopher, S. A., J. Chou, J. Zhang, X. Li, and R. M. Welch, Shortwave direct radiative forcing of biomass burning aerosols estimated from VIRS and CERES, *Geophys. Res. Lett.*, **27**(15), 2197-2200, 2000a.
- Christopher, S. A., X. Li, R. M. Welch, P. V. Hobbs, J. S. Reid, and T. F. Eck, Estimation of downward and top-of-atmosphere shortwave irradiances in biomass burning regions during SCAR-B, *J. Appl. Meteorol.*, **39**, 1742-1753, 2000b.
- Chu, D. A., Y. J. Kaufman, L. A. Remer, and B. N. Holben, Remote sensing of smoke from MODIS airborne simulator during the SCAR-B experiment, *J. Geophys. Res.*, **103**, 31,979-31,987, 1998.
- Deuze, J. L., F. M. Breon, P. Y. Deschamps, C. Devaux, M. Herman, A. Podaire, and J. L. Roujean, 1993: Analysis of the POLDER (Polarization and Directionality of Earth's Reflectances) airborne instrument observations over land surfaces, *Remote Sens. Environ.*, **45**, 137-154, 1993.
- D'Almeida, G. A., K. Koepke, and E. R. Shettle, *Atmospheric Aerosol: Global Climatology and Radiative Characteristics*, A. Deepak, Hampton, Va., 1991.
- Eck, T. F., B. N. Holben, J. S. Reid, O. Dubovik, A. Smirnov, N. T. O'Neill, I. Slutsker, and S. Kinne, Wavelength dependence of the optical depth of biomass burning, urban, and dust aerosols, *J. Geophys. Res.*, **104**, 31,333-31,349, 1999.
- Ellrod, G. P., R. V. Achutnui, J. M. Daniels, E. M. Prins, and J. P. Nelson III, An assessment of GOES 8 imager data quality, *Bull. Am. Meteorol. Soc.*, **78**, 1971-1983, 1998.
- Ferek, R. J., J. S. Reid, P. V. Hobbs, D. R. Blake, and C. Liousse, Emission Factors of hydrocarbons, halocarbons, trace gases, and particles from biomass burning in Brazil, *J. Geophys. Res.*, **103**, 32,107-32,118, 1998.
- Fraser, R. S., and Y. J. Kaufman, Calibration of satellite sensors after launch, *Appl. Optics*, **25**, 1177-1185, 1986.
- Greenwald T. J., and S. A. Christopher, Daytime variation of marine

- stratocumulus properties as observed from Geostationary Satellite, *Geophys. Res. Lett.*, **26**, 1723-1726, 1999.
- Greenwald, T. J., and S. A. Christopher, The GOES-IM Imagers: New tools for studying the microphysical properties of boundary layers clouds, *Bull. Am. Meteorol. Soc.*, **81**, 2607-2619, 2000.
- Greenwald, T. J., S. A. Christopher, and J. Chou, Cloud liquid water path comparisons from passive microwave and solar reflectance satellite measurements: Assessment of sub-field-of-view cloud effects in microwave retrievals, *J. Geophys. Res.*, **102**, 19,585-19,597, 1997.
- Hansen, J., M. Sato, A. Lacis, and R. Ruedy, The missing climate force, *Philos. Trans. R. Soc. London*, **352**, 231-240, 1997.
- Hao, W. M., and M. H. Liu, Spatial and temporal distribution of biomass burning, *Global Biogeochem. Cycles*, **8**, 495-503, 1994.
- Holben, B. N., A. Setzer, T. F. Eck, A. Pereira, and I. Slutsker, Effect of dry season biomass burning on Amazon basin aerosol concentrations and optical properties, 1992-1994, *J. Geophys. Res.*, **101**, 19,465-19,481, 1996.
- Holben, B. N., T. F. Eck, I. Slutsker, D. Tanre, J. P. Buis, A. Setzer, E. Vermote, J. A. Reagan, Y. J. Kaufman, T. Nakajima, F. Lavenue, I. Jankowiak, and A. Smirnov, AERONET - A Federated Instrument Network and Data Archive for aerosol characterization, *Remote Sens. Environ.*, **66**, 1-16, 1998.
- Hsu, N. C., J. R. Herman, P. K. Bhartia, C. J. Seftor, O. Torres, A. M. Thompson, J. F. Gleason, T. F. Eck, and B. N. Holben, Detection of biomass burning smoke from TOMS measurements, *Geophys. Res. Lett.*, **23**, 745-748, 1996.
- Kaufman, Y. J., Measurements of the aerosol optical thickness and the parth radiance-Implications on aerosol remote sensing and atmospheric corrections, *J. Geophys. Res.*, **98**, 2677-2692, 1993.
- Kaufman, Y. J., and R. S. Fraser, Confirmation of the smoke particles effect on cloud and climate, *Science*, **277**, 1636-1639, 1997.
- Kaufman, Y. J., A. Setzer, D. Ward., D. Tanre, B. N. Holben, P. Menzel, M. C. Pereira, and R. Rasmussen, Biomass burning airborne and spaceborne experiment in the Amazonas (BASE A), *J. Geophys. Res.*, **97**, 14,581-14,599, 1992.
- King, M. D., Y. J. Kaufman, D. Tanre, and T. Nakajima, Remote sensing of tropospheric aerosols from space: past, present and future, *Bull. Am. Meteorol. Soc.*, **80**, 2229-2287, 1999.
- Knapp, K., and T. Vonder Haar, Calibration of the eighth Geostationary Operational Environmental Satellite (GOES 8) imager visible sensor, *J. Atmos. Oceanic Technol.*, **17**, 1639-1644, 2000.
- Martins, J. V., P. V. Hobbs, R. E. Weiss, and P. Artaxo, Sphericity and morphology of smoke particles from biomass burning in Brazil, *J. Geophys. Res.*, **103**, 32,051-32,058, 1998.
- McClatchey, R. A., R. W. Fenn, J. E. A. Selby, F. E. Volz, and J. S. Garing, *Optical Properties of the Atmosphere*. 3rd ed., AFCRL Environ. Res. Pap. no. 411, 108 pp., 1972.
- McDow, S. R., M. Jang, Y. Hong, and R. M. Kamens, An approach to studying the effect of organic composition on the atmospheric aerosol photochemistry, *J. Geophys. Res.*, **101**, 19,593-19,600, 1996.
- Menzel, W. P., and J. F. W. Purdom, Introducing GOES-I: The first of a new generation of Geostationary Operational Environmental Satellites, *Bull. Am. Meteorol. Soc.*, **75**, 757-781, 1994.
- Nguyen, L., P. Minnis, J. K. Ayers, W. L. Smith Jr., and Shu-Peng Ho, Intercalibration of geostationary and polar satellite imager data using AVHRR, VIRS, and ASTR-2 data, *preprints, 10th Conference on Atmospheric Radiation*, Madison, Wisc., Am. Meteorol. Soc., 405-408, 1999.
- Penner, J. E., R. E. Dickinson, and C. A. O'Neill, Effects of aerosol from biomass burning on the global radiation budget, *Science*, **256**, 1432-1434, 1992.
- Pereira, E. B., A. W. Setzer, F. Gerab, P. E. Artaxo, M. C. Pereira, and G. Monroe, Airborne measurements of aerosols from burning biomass in Brazil related to the TRACE A experiment, *J. Geophys. Res.*, **101**, 23,983-23,992, 1996.
- Pincus, R., M. A. Baker, and C. S. Bretherton, What controls stratocumulus radiative properties? Lagrangian observations of cloud evolution, *J. Atmos. Sci.*, **54**, 2215-2236, 1997.
- Prins, E. M., J. M. Feltz, W. P. Menzel, and D. E. Ward, An overview of GOES-diurnal fire and smoke results for SCAR-B and the 1995 fire season in South America, *J. Geophys. Res.*, **103**, 31,821-31,836, 1998.
- Rao, C. R. N., J. Chen, and N. Zhang, Calibration of the visible channel of the GOES imager using the advanced very high resolution radiometer, *preprints, 10th Conference on Atmospheric Radiation*, Madison, Wisc., Am. Meteorol. Soc., 560-563, 1999.
- Reid, J. S., and P. V. Hobbs, Physical and optical properties of young smoke from individual biomass fires in Brazil, *J. Geophys. Res.*, **103**, 32,013-32,030, 1998a.
- Reid, J. S., P. V. Hobbs, R. J. Ferek, D. R. Blake, J. V. Martins, M. R. Dunlap, and C. Liousse, Physical, chemical and optical properties of regional hazes dominated by smoke in Brazil, *J. Geophys. Res.*, **103**, 32,059-32,080, 1998b.
- Reid, J. S., T. Eck, S. A. Christopher, B. Holben, and P. Hobbs, Use of the Angstrom exponent to estimate the variability of optical and physical properties of aging smoke particles in Brazil, *J. Geophys. Res.*, **104**, 27,473-27,490, 1999.
- Remer, L. A., Y. J. Kaufman, B. N. Holben, A. M. Thompson, and D. McNamara, Biomass burning aerosol size distribution and modeled optical properties, *J. Geophys. Res.*, **103**, 31,879-31,892, 1998.
- Ricchiazzi, P., S. Yang, C. Gautier, and D. Sowle, SBDART: A research and teaching software tool for plane-parallel radiative transfer in the Earth's atmosphere, *Bull. Am. Meteorol. Soc.*, **79**, 2101-2114, 1998.
- Ross, J. L., P. V. Hobbs, and B. Holben, Radiative characteristics of regional hazes dominated by smoke from biomass burning in Brazil: Closure tests and direct radiative forcing, *J. Geophys. Res.*, **103**, 31,925-31,941, 1998.
- Simirnov, A., B. N. Holben, T. F. Eck, O. Dubovik, and I. Slutsker, Cloud screening and quality control algorithms for the AERONET database, *Remote Sens. Environ.*, **73**, 337-349, 2000.
- Stowe, L. L., A. M. Ignatov, and R. R. Singh, Development, validation, and potential enhancements to the second-generation operational aerosol product at the National Environmental Satellite, Data, and Information Service of the National Oceanic and Atmospheric Administration, *J. Geophys. Res.*, **102**, 16,923-16,934, 1997.
- Weinreb, M. P., M. Jamison, N. Fulton, Y. Chen, J. X. Johnson, J. Bremer, C. Smith, and J. Baucum, Operational calibration of Geostationary Operational Environmental Satellite 8 and 9 imagers and sounders, *Appl. Opt.*, **36**, 6895-6904, 1997.

S. A. Christopher (corresponding author) and J. Zhang, Department of Atmospheric Sciences, University of Alabama in Huntsville, Huntsville, AL 35806 (sundar@nsstc.uah.edu).

B. N. Holben, Biospheric Sciences Branch, Code 923, NASA Goddard Space Flight Center, Greenbelt, MD 20771.

(Received March 23, 2000; revised June 29, 2000; accepted August 22, 2000.)